

# The small-world effect is a modern phenomenon

Seth A. Marvel,<sup>1</sup> Travis Martin,<sup>2</sup> Charles R. Doering,<sup>1,3</sup> David Lusseau,<sup>4</sup> and M. E. J. Newman<sup>3</sup>

<sup>1</sup>*Department of Mathematics, University of Michigan, Ann Arbor, MI 48109, U.S.A.*

<sup>2</sup>*Department of Electrical Engineering and Computer Science,  
University of Michigan, Ann Arbor, MI 48109, U.S.A.*

<sup>3</sup>*Department of Physics and Center for the Study of Complex Systems,  
University of Michigan, Ann Arbor, MI 48109, U.S.A.*

<sup>4</sup>*Institute of Biological and Environmental Sciences, University of Aberdeen, Aberdeen, U.K.*

The “small-world effect” is the observation that one can find a short chain of acquaintances, often of no more than a handful of individuals, connecting almost any two people on the planet. It is often expressed in the language of networks, where it is equivalent to the statement that most pairs of individuals are connected by a short path through the acquaintance network. Although the small-world effect is well-established empirically for contemporary social networks, we argue here that it is a relatively recent phenomenon, arising only in the last few hundred years: for most of mankind’s tenure on Earth the social world was large, with most pairs of individuals connected by relatively long chains of acquaintances, if at all. Our conclusions are based on observations about the spread of diseases, which travel over contact networks between individuals and whose dynamics can give us clues to the structure of those networks even when direct network measurements are not available. As an example we consider the spread of the Black Death in 14th-century Europe, which is known to have traveled across the continent in well-defined waves of infection over the course of several years. Using established epidemiological models, we show that such wave-like behavior can occur only if contacts between individuals living far apart are exponentially rare. We further show that if long-distance contacts are exponentially rare, then the shortest chain of contacts between distant individuals is on average a long one. The observation of the wave-like spread of a disease like the Black Death thus implies a network without the small-world effect.

## I. INTRODUCTION

The *small-world effect* is the observation that it is possible to connect almost any two members of the world population by a short chain of acquaintances. In network terms, the average length of the shortest path between two nodes in a social network is small. In practice, “small” usually means less than about a dozen steps, even when the network has billions of members. Scientific studies of the small-world effect began in the 1950s with mathematical work by Pool and Kochen [1], which inspired a now-famous series of experiments by Milgram and co-workers [2, 3]. Recent years have seen a resurgence of interest in the topic following publication of an influential paper by Watts and Strogatz [4], and many experiments have been performed directly confirming the existence of the small-world effect by explicitly measuring path lengths in networks [5–9].

Given the extensive documentation of the small-world effect, one might consider it to be an established fact. It would not be unreasonable to assume, based on the published literature, that essentially all social networks exhibit the effect. Here we argue, however, that this is not the case. In particular, we present historical observations and mathematical results that together suggest that path lengths in social networks used to be much longer than they are today. The small-world effect is, we contend, a modern phenomenon.

Explicit studies of the structure of social networks go back only about a century—the work of psychologist Jacob Moreno [10] in the 1930s is considered one of the

earliest examples—so we have no direct measurements of pre-industrial networks. Instead, therefore, our conclusions in this paper are based on historical patterns of the spread of disease. Many diseases are passed between individuals via close contact, be it through shared air, animal vectors, sexual contact, or other means of transmission. The pattern of contacts forms a network whose structure in turn dictates the pattern of infection and hence observations of diseases can give us hints about network structure. The physical contact networks governing disease are not in general the same as acquaintance networks or social contact networks. But, to the extent that most social exchange among humans before the modern era took place via face-to-face interaction, the network of social contacts was, to a good approximation, a subset of the network of physical contacts, and this observation allows us to draw conclusions about social networks as well.

Like other networks, physical contact networks in the modern world appear to show the small-world effect. Work on human mobility has shown that the lengths of trips people take follow a power-law distribution over a wide range of scales from tens to thousands of kilometers [11, 12], and theoretical work by Kleinberg [13] suggests that such a power-law distribution of connections implies the small-world effect. Moreover, new strains of pathogens such as influenza are observed to travel around the globe rapidly, appearing in distant locations almost simultaneously [14]. One possible cause of such rapid spread is the presence of short chains of physical contacts linking individuals in distant parts of the world.

Historically, however, diseases have spread much

slower, which raises the possibility that short contact chains spanning long distances did not exist, or were much rarer, before the modern era. But the mere absence of rapid disease spreading is not, on its own, conclusive. In their work on the small-world effect, Watts and Strogatz [4] showed that only a vanishing fraction of long-distance trips are necessary to achieve the effect, in which case it is conceivable that the ancient world was small. Some long-range connections have existed as far back as reliable records of civilization extend, being vital to the communication and intelligence gathering networks of early empires and a necessary part of intercontinental trade [15]. The question we need to answer, therefore, is whether there were enough of these long-range connections to produce a small-world effect in historical contact networks. In this paper, we argue that there were not.

## II. OUTLINE OF ARGUMENT

One can make a heuristic argument for the historical absence of the small-world effect as follows. The small-world effect is usually defined formally as the observation that the typical network path length between individuals in a population increases no faster than logarithmically with population size. Conversely, this implies that the average number of individuals a given distance away from a randomly chosen starting point in the network increases exponentially with distance. And this in turn suggests that a disease spreading outward from an initial carrier will infect an exponentially growing number of people as time passes until the infection saturates the population. Such exponential growth has been observed in modern-day disease outbreaks [16]. Many historical outbreaks, on the other hand, show a convincingly non-exponential pattern of spread—see Fig. 1 for an example—which suggests that the small-world effect was not present at the time these epidemics occurred. While this argument is intuitive, however, it is difficult to make rigorous, so in this paper we take a different approach, based not on temporal disease patterns but on spatial ones. In outline, our argument is as follows.

Our key empirical observation is that, while modern-day epidemics spread easily and rapidly across vast distances, the same is not true of historical ones. Historical epidemics often advanced across the landscape in a measured, wave-like fashion. We will focus especially on one particular example, the 14th-century pandemic known as the Black Death (Fig. 1). An unusually destructive outbreak, the Black Death is thought to have begun in China and then spread along the Silk Road to the Levant. From there it was carried on trade ships along the Mediterranean and, starting in 1347, spread northward across the European continent, reaching France and Austria in 1348, Germany in 1349, and Scandinavia and Russia in 1350 [17]. As Fig. 1 illustrates, the epidemic displayed a well-defined wave-front of infection that traveled across the landscape at a speed of about 800 kilometers per year.

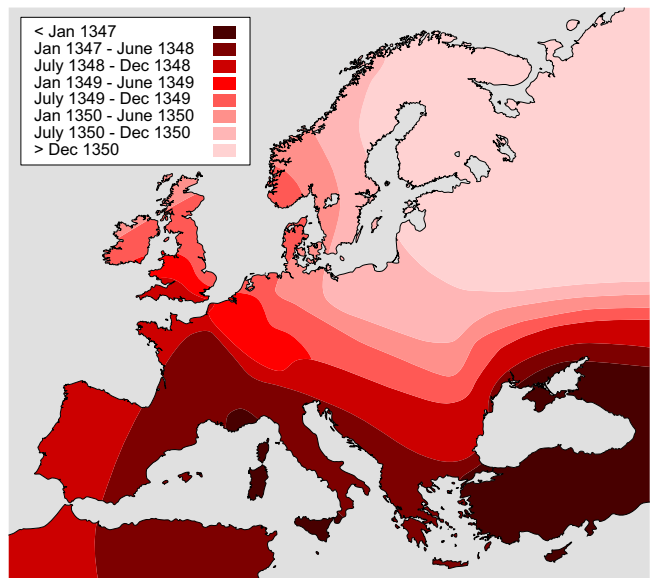


FIG. 1: The spread of the Black Death across Europe in the 14th century, after Sherman and Salisbury [18]. Observe that the disease advanced as a wave of infection across the continent at a more or less constant speed for over three years.

Now consider Fig. 2, which shows the results of two different computer simulations of the spread of a disease through a population. The population density is the same in both simulations, as is the average probability of disease transmission between individuals, yet the two simulations look very different. In the first simulation (panel A) the disease spreads outward in a circular fashion from an initial seed in the center, creating a clear wave-like front. In the second (panel B) the spread is irregular, with many different centers of infection and no clear leading edge, even though this simulation also was started from a single central seed. The crucial difference between the two simulations lies in the probability of disease transmission between individuals as a function of distance. In the first simulation, probability of transmission falls off exponentially with distance (i.e., quite rapidly), whereas in the second it falls off more slowly, following a power law, with a fat tail of occasional long-distance transmission events that are responsible for the satellite outbreaks away from the center of the figure.

It turns out that the behavior of the disease in these two cases is not merely quantitatively different, but also qualitatively so. No matter how long the first simulation is allowed to continue, it will always display a distinct wave-front (provided we give the disease an arbitrarily large space to expand into). By contrast, the irregular nature of the second simulation only becomes more dramatic as time goes by, and eventually all similarity to wave-like spread is lost. While the results of Fig. 2 are numerical only, we will demonstrate these conclusions analytically in the following sections.

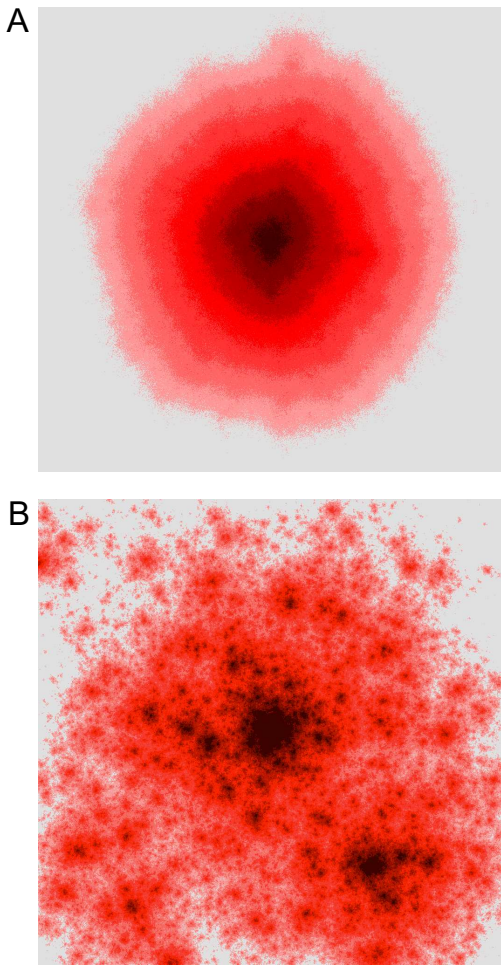


FIG. 2: Simulations of the spatial spread of an susceptible–infectious (SI) epidemic on a  $1000 \times 1000$  grid according to the model in this paper. Each simulation was initiated with a single carrier in the center of the system and colors represent the time at which each node contracted the disease. The contact kernel for (A) is an exponential  $\alpha(r) = ae^{-br}$ . For (B) it is a power-law  $\alpha(r) = r^{-\gamma}$  with  $r$  restricted to be greater than some minimum value  $r_{\min}$  to eliminate infinities. As the figure shows, the exponential kernel gives rise to a distinct wave-front of disease propagating out from the center while the power-law kernel produces a more nonlocal spread of disease, with many satellite outbreaks and no clear wave-front.

We will show using a well-established model of the spreading process that an epidemic can exhibit wave-like spread at constant speed only if the probability of disease-causing contact between pairs of individuals falls off exponentially, or faster, with the distance between them. We then employ this result as the input to an analysis of the network of physical contacts between individuals. We show that if indeed probability of contact falls off exponentially with distance, then typical path lengths in the contact network are long and the network does not display the small-world effect. Furthermore, if

the network of *social* contacts is, as we have said, a subset of the network of physical contacts, then the social contact network is also not a small world, since the social network is formed by removing edges from the physical network, which can only make paths longer, not shorter.

Given the observation of wave-like spread of the Black Death, we therefore conclude, subject to the assumptions made in the analysis, that the social contact network within Europe in the 14th century did not display the small-world effect.

### III. EPIDEMIC WAVE-FRONTS IMPLY RARE LONG-RANGE CONTACTS

In this and the following section, we present detailed arguments supporting the claims made above. Our arguments are based on mathematical modeling of the geographic spread of disease. We consider a model in which a disease spreads through a population of individuals each of whom lives at some particular geographic location. Since the transmission of disease between individuals normally requires close physical proximity, it can only take place if one individual travels from his or her location to the location of another, or if both travel to the same third point. Our model uses a *contact kernel* to specify the average frequency of such contacts as a function of where the two individuals live. For simplicity we take this kernel to be isotropic (the frequency of meetings is independent of compass direction) and translation invariant (the same in all parts of the world), so that it is a function only of the distance  $r$  between individuals. We also assume that average frequency of contact falls off with distance beyond some point, so the kernel is nonincreasing for all  $r$  greater than some nonnegative constant  $R$ .

As an illustration of a contact kernel, consider again the Black Death. The etiology of the Black Death has been the subject of some debate, but the current consensus, based in part on DNA evidence from mass graves, is that it was an outbreak of bubonic plague, which is caused by the bacterium *Y. pestis* and communicated both directly from person to person and by rats and fleas [19]. Neither fleas nor rats travel long distances, however, other than when they are carried by human transportation, so the contact network over which the disease is transmitted consists of primarily local contacts plus longer range contacts that mirror those of the human population [11]. The contact kernel combines these different transmission vectors and transportation processes into a single quantity that we take as an input to our model.

We also need to model the dynamics of disease spreading. There are a number of established mathematical models for the spatial spread of epidemics, perhaps the most widely studied being diffusion models based on the Fisher–Kolmogorov–Petrovsky–Piskunov family of equations. These models are inadequate to represent the phenomena we are interested in, because diffusion is an in-

herently local process, equivalent to a disease transmission process with contacts that span infinitesimal distances only. To represent the nonlocal transmission implied by our contact kernel, we use the model of Mollison [20], which is a spatial but nonlocal susceptible–infectious (SI) model defined as follows.

Let  $P(\mathbf{u}, t)$  be the probability that an individual at position  $\mathbf{u}$  has the disease at time  $t$  and let  $\alpha(r)$  be the contact kernel, defined as the probability per unit time and area that an individual has contact sufficient to contract the disease from another a distance  $r$  away (although transmission will only actually occur if the first individual does not have the disease and the second does). For simplicity we will assume our population to be uniformly distributed in two-dimensional space. Real populations are not uniformly distributed, being concentrated in population centers like towns and villages, and this could in principle impact travel patterns and hence the spread of disease, but we will neglect those effects here. Then the dynamics of the resulting epidemic is governed by the integro-differential equation [20],

$$\frac{\partial}{\partial t}P(\mathbf{u}, t) = [1 - P(\mathbf{u}, t)] \int \alpha(|\mathbf{u} - \mathbf{v}|)P(\mathbf{v}, t) d^2\mathbf{v}. \quad (1)$$

The leading factor on the right represents the probability that an individual at position  $\mathbf{u}$  is uninfected at time  $t$  and the integral represents the probability of becoming newly infected by an individual somewhere else in the plane. The equation can be regarded as a continuous-space approximation to the exact dynamics in a discrete population on, for example, a square grid, where the integral extends over the grid area.

Analysis of Eq. (1) is more complicated than for diffusive models because of its nonlocality; standard techniques for partial differential equations cannot be directly applied. Fortunately, however, we do not need to solve the equation in complete generality. Our goal is only to determine whether wave-like solutions, of the kind seen in the spread of the Black Death, are possible, and this question turns out to be a tractable one.

Consider a potential solution to Eq. (1) taking the form of a traveling wave with velocity  $v$ . Without loss of generality, assume the wave to be traveling in the positive  $x$  direction so that, writing  $\mathbf{u} = (x, y)$ , we have  $P(\mathbf{u}, t) = f(x - vt)$  for some function  $f$  in the range  $0 \leq f \leq 1$ . Substituting into Eq. (1), we obtain

$$-v \frac{df}{dx} = [1 - f(x)] \int_{-\infty}^{\infty} \beta(x' - x)f(x') dx', \quad (2)$$

where

$$\beta(x) = \int_{-\infty}^{\infty} \alpha(\sqrt{x^2 + y^2}) dy. \quad (3)$$

From the properties of the contact kernel discussed earlier,  $\beta$  is nonnegative, integrable, symmetric about the origin, and nonincreasing for  $x > R$ .

The mathematical question we wish to answer is this: what is implied about  $\alpha$  if a solution  $0 < f(x) < 1$  to Eq. (2) exists? In plain terms, if we encounter an epidemic with a stable, steadily advancing wave-front, what does that tell us about the underlying contact kernel? Mollison [20] showed that if a solution to the equation exists, then the integral of the tail of  $\beta$  decays exponentially or faster. Our first theorem is similar in spirit to this result, but different in detail and with a more straightforward proof.

**Theorem 1:** If Eq. (2) has a solution  $0 < f(x) < 1$ , then  $\alpha(r) = O(e^{-cr})$  in the limit  $r \rightarrow \infty$ , where  $c = (1/\sqrt{2}v) \int_0^{\infty} \beta(x) dx$ .

**Proof:** Equation (2) and the condition that  $0 < f < 1$  imply that  $f$  is continuous (since  $f'(x)$  is bounded) and decreasing (since  $f'(x) < 0$ ).

i) Using these facts, we can compute an upper bound on  $f(x)$  for  $x > 0$ . We note that the integral in Eq. (2) only decreases (or stays the same) if we restrict the domain of integration to the interval  $(-\infty, x)$  and then replace  $f(x')$  with  $f(x)$  (because  $f(x)$  is decreasing in  $x$ ). Making these changes and then changing the integration variable to  $z = x' - x$ , we find

$$-v \frac{df}{dx} \geq [1 - f(x)]f(x) \int_0^{\infty} \beta(z) dz, \quad (4)$$

where we have made use of the fact that  $\beta$  is symmetric about the origin. Equation (2) is translation invariant, so without loss of generality we will let  $f(0) = \frac{1}{2}$ . Separating variables in (4) and integrating from 0 to  $x$  then gives  $f(x) \leq (1 + e^{bx})^{-1}$  for  $x \geq 0$ , where  $b = v^{-1} \int_0^{\infty} \beta(z) dz$ . Thus  $f(x)$  obeys the strict inequality

$$f(x) < e^{-bx} \quad \text{for } x > 0. \quad (5)$$

In other words, the leading edge of the epidemic decays exponentially or faster.

ii) We now use this result to place bounds on the behavior of  $\beta(x)$  for large  $x$ . To do this we divide Eq. (2) by  $1 - f(x)$  and integrate from  $x$  to  $\infty$  to obtain

$$-v \ln[1 - f(x)] = \int_x^{\infty} \int_{-\infty}^{\infty} \beta(z - x')f(z) dz dx'. \quad (6)$$

Performing a Taylor expansion of the left-hand side about  $f = 0$  and applying (5), we arrive at the asymptotic upper bound

$$-v \ln[1 - f(x)] \lesssim ve^{-bx} \quad \text{as } x \rightarrow \infty, \quad (7)$$

where  $g(x) \lesssim h(x)$  means that for any  $\epsilon > 0$  there is an  $X < \infty$  such that  $g(x) < (1 + \epsilon)h(x)$  for all  $x > X$ .

Now we restrict the interior integral on the right-hand side of (6) to the interval  $(-\infty, 0)$  and replace  $f(z)$  with its smallest value in that interval, which is  $f(0) = \frac{1}{2}$ .

Making a change of variables in the inner integral and noting that  $\beta$  is even, we obtain the inequality

$$\int_x^\infty \int_{-\infty}^\infty \beta(z-x')f(z) dz dx' \geq \frac{1}{2} \int_x^\infty \int_{x'}^\infty \beta(z) dz dx'. \quad (8)$$

Then (6), (7), and (8) together imply that

$$\int_x^\infty \int_{x'}^\infty \beta(z) dz dx' \lesssim 2ve^{-bx}. \quad (9)$$

iii) This is not yet quite the result we need. It gives us a bound on a double integral of  $\beta$ . Our next step gives a bound on  $\beta(x)$  itself.

Let  $\lambda$  be a positive constant. As we have said,  $\beta(x)$  is nonincreasing for  $x > R$ , so the rectangle of height  $\beta(x+\lambda)$  from any  $x > R$  to  $x+\lambda$  lies under the nonincreasing curve of  $\beta(x)$ . Hence,  $\lambda\beta(x+\lambda) \leq \int_x^\infty \beta(x') dx'$  and, setting  $\lambda = 1/b$ , we have

$$\frac{1}{b}\beta(x+1/b) \leq \int_x^\infty \beta(x') dx'. \quad (10)$$

Noting that  $\int_x^\infty \beta(x') dx'$  is also a nonincreasing function of  $x$  for all  $x$  (since  $\beta(x)$  is nonnegative everywhere), we can repeat the same argument again to show that

$$\frac{1}{b} \int_{x+1/b}^\infty \beta(x') dx' \leq \int_x^\infty \int_{x'}^\infty \beta(z) dz dx'. \quad (11)$$

Then making the substitution  $x \rightarrow x+1/b$  in (10) and combining with (11) we have

$$\frac{1}{b^2}\beta(x+2/b) \leq \int_x^\infty \int_{x'}^\infty \beta(z) dz dx'. \quad (12)$$

Along with (9) this now yields an asymptotic upper bound on  $\beta(x)$  itself:

$$\beta(x) \lesssim 2vb^2e^2 e^{-bx}. \quad (13)$$

iv) The final step in our proof converts this upper bound on  $\beta(x)$  to an upper bound on the contact kernel  $\alpha(r)$ . From (13) and the definition of  $\beta(x)$ , Eq. (3), we have

$$\int_{-\infty}^\infty \alpha(\sqrt{x^2+y^2}) dy \lesssim 2vb^2e^2 e^{-bx}. \quad (14)$$

Integrating both sides with respect to  $x$  from an arbitrary  $r > R$  to  $\infty$ , we obtain

$$\int_r^\infty \int_{-\infty}^\infty \alpha(\sqrt{x^2+y^2}) dy dx \lesssim 2vbe^2 e^{-br}. \quad (15)$$

(Note that the definition of  $\lesssim$  permits this.) The domain of the double integral in this expression is the region  $D = \{(x, y) \mid r \leq x < \infty, -\infty < y < \infty\}$ . The union of four copies of  $D$ , rotated about the origin by  $0, \pi/2, \pi,$  and  $3\pi/2$ , contains the polar region  $P = \{(r', \theta) \mid \sqrt{2}r \leq r' < \infty, 0 \leq \theta < 2\pi\}$ . So if we integrate  $\alpha$  over these four

copies of  $D$  and sum the results, the sum will be as large or larger than the integral of  $\alpha$  over  $P$ :

$$4 \int_r^\infty \int_{-\infty}^\infty \alpha(\sqrt{x^2+y^2}) dy dx \geq 2\pi \int_{\sqrt{2}r}^\infty \alpha(r') r' dr'. \quad (16)$$

Observing that  $r'\alpha(r') > R\alpha(r')$  for all  $r' > R$  and that  $\alpha(r')$  is nonincreasing in this regime, we now integrate from  $\sqrt{2}r$  to  $\infty$  and apply the same argument as for (10) to obtain

$$\int_{\sqrt{2}r}^\infty \alpha(r') r' dr' > \frac{\sqrt{2}R}{b}\alpha(\sqrt{2}r + \sqrt{2}/b). \quad (17)$$

Then combining (15), (16), and (17) we have

$$\alpha(r) \lesssim \frac{4\sqrt{2}vc^2e^3}{\pi R} e^{-cr}, \quad (18)$$

where  $c = b/\sqrt{2} = (1/\sqrt{2}v) \int_0^\infty \beta(x) dx$ . This completes the proof.  $\square$

This result helps explain the behavior we observed in Fig. 2. In the first panel we observe distinct, wave-like spread of the disease from the initial point of infection, and under these circumstances Theorem 1 tells us that the underlying infection kernel must have exponential (or faster) decay at long distances, which is correct in this case. Conversely, the theorem tells us that if the kernel decays slower than an exponential at long distances, then we will not observe wave-like spread, which agrees with the results shown in the second panel of the figure.

#### IV. RARE LONG-RANGE CONTACTS IMPLY NO SMALL-WORLD EFFECT

Given that wave-like behavior implies a contact kernel decaying at least as fast as an exponential, what now can we conclude about the shape of the network of disease-causing contacts? We show in this section that the network must be a ‘‘large world,’’ by which we mean that it does not show the small-world effect. The most widely accepted formal definition of the small-world effect is that typical path lengths in a network increase with the number of nodes  $n$  no faster than  $\log n$  [21, 22], and we will adopt that definition here. Studies, both theoretical and empirical, suggest that many networks satisfy this definition and hence display the small-world effect, but we will show that an exponential contact kernel produces path lengths that increase significantly faster, roughly as  $\sqrt{n}/\log n$ .

It is important to emphasize that the small-world effect is a mathematical statement about scaling relationships between path lengths and population size, not a statement about how path lengths have changed in practice as the population of the world has grown. The population of the Earth has increased during most of human history and that increase has been accompanied by increases in population density, changes in living conditions

and social customs, and improvements in technology, including technology for travel and communication. All of these factors could affect the shape of social networks and hence might potentially change path lengths between individuals. But it is not this process that the small-world effect describes. The small-world effect says that even if all other factors were kept fixed (such as population density, social customs, and technology), typical path lengths between individuals in the social network would still increase at most logarithmically with population. This is the sense in which we use the phrase.

To demonstrate our results we first need to define exactly what network we are considering. We have so far avoided direct reference to the contact network by working in the continuous space of Eq. (1), which, as we have said, can be thought of as a continuous approximation to the disease dynamics of a discrete population. To address the structure of the network, we return to the discrete view and consider a population of  $n$  individuals uniformly distributed in two-dimensional space. For simplicity, let us choose  $n$  to be a perfect square and place our  $n$  individuals at the sites of an  $\sqrt{n} \times \sqrt{n}$  regular square lattice with unit lattice spacing (though the structure of our argument is not sensitive to the exact choice of positions for the population members).

We then place edges between individuals in the population to represent the physical contacts by which disease is or could be transmitted. We place a total of exactly  $\gamma n$  edges, where  $2\gamma$  is the mean degree of the network—the mean number of connections an individual has. In keeping with our assumption above that all social and other parameters are held constant, we will assume that the mean degree remains constant as  $n$  is varied. The position of each of the  $\gamma n$  edges is drawn independently from the same probability distribution  $p_n(\mathbf{u}, \mathbf{v})$ , meaning that the ends of an edge fall at positions  $\mathbf{u}$  and  $\mathbf{v}$  with probability  $p_n(\mathbf{u}, \mathbf{v})$ . The form of  $p_n(\mathbf{u}, \mathbf{v})$  depends on  $n$ , but if the edges represent physical contacts then it must assume the same functional form as the contact kernel  $\alpha(|\mathbf{v} - \mathbf{u}|)$  in the limit of large system size. Since  $p_n(\mathbf{u}, \mathbf{v})$  must be normalized so that  $\sum_{\mathbf{u}, \mathbf{v}} p_n(\mathbf{u}, \mathbf{v}) = 1$ , we then have

$$p_n(\mathbf{u}, \mathbf{v}) \leq \frac{\kappa}{n} \alpha(|\mathbf{v} - \mathbf{u}|), \quad (19)$$

for some constant  $\kappa$  and sufficient large  $n$ , given that the contact kernel is integrable.

We also place additional edges between all pairs of nearest neighbors on the lattice, which ensures that a path exists between every pair of lattice sites and simplifies our proof. These edges need not represent real physical interactions and do not qualitatively affect our final result—clearly their addition can only reduce path lengths in the network, not increase them, so if there is no small-world effect when they are included then there can be no small-world effect without them either. Similar nearest-neighbor edges have been used in other models of the small-world effect [13, 23], and models of this kind, consisting of a lattice of nearest-neighbor connections

plus random longer-range ones, are generically known as “small-world models” [4].

Now consider a pair of sites on the lattice separated by geographic distance of order the linear dimension  $\sqrt{n}$ , which we will write as  $q\sqrt{n}$  for some constant  $q > 0$ . For instance we might choose a pair of sites a distance  $\frac{1}{2}\sqrt{n}$  apart. (Without this requirement one could trivially find a short path between sites by choosing sites that just happened to be very close together.) Let  $L_n$  be the number of hops in the shortest network path between these sites in a particular realization of the network and let  $E[L_n]$  be the expected value of  $L_n$  over all realizations.

**Theorem 2:** If  $\alpha(r) = O(e^{-cr})$  in the limit  $r \rightarrow \infty$  for some constant  $c$ , then  $E[L_n] = \Omega(\sqrt{n}/\log n)$  in the limit  $n \rightarrow \infty$ . Informally, the expected distance between sites is at least a constant times  $\sqrt{n}/\log n$  in the limit.

**Proof:** Let  $\mathcal{E}$  be the set of edges in a particular realization of our model and let  $(\mathbf{u}, \mathbf{v}) \in \mathcal{E}$  indicate that there is an edge between the sites at positions  $\mathbf{u}$  and  $\mathbf{v}$ . On a finite lattice there is necessarily, somewhere in the network, an edge or edges that span the largest geographic distance, and hence for any length  $\ell(n) \geq 1$  that we choose there is a well-defined probability  $\Pr[\forall (\mathbf{u}, \mathbf{v}) \in \mathcal{E} : |\mathbf{u} - \mathbf{v}| \leq \ell(n)]$  that all edges will be less than or equal to  $\ell(n)$  in length. Moreover, if no edge is longer than  $\ell(n)$ , then the number of hops  $L_n$  in the shortest network path between our two sites of interest is at least as great as for a path connecting the same two sites and composed entirely of hops of length  $\ell(n)$ . In other words  $L_n \geq q\sqrt{n}/\ell(n)$ . Combining these observations, it follows that

$$\Pr[L_n \geq q\sqrt{n}/\ell(n)] \geq \Pr[\forall (\mathbf{u}, \mathbf{v}) \in \mathcal{E} : |\mathbf{u} - \mathbf{v}| \leq \ell(n)]. \quad (20)$$

Applying Markov’s inequality to the left-hand side we have

$$\Pr[L_n \geq q\sqrt{n}/\ell(n)] \leq \frac{\ell(n)}{q\sqrt{n}} E[L_n], \quad (21)$$

and combining this result with (20) gives

$$E[L_n] \geq \frac{q\sqrt{n}}{\ell(n)} \Pr[\forall (\mathbf{u}, \mathbf{v}) \in \mathcal{E} : |\mathbf{u} - \mathbf{v}| \leq \ell(n)]. \quad (22)$$

The function  $\ell(n)$  is undetermined in this expression. We now show that if we choose  $\ell(n)$  proportional to  $\log n$  then the probability on the right-hand side of (22) is nonzero in the limit  $n \rightarrow \infty$ , and hence that  $E[L_n]$  grows at least as fast as  $\sqrt{n}/\log n$ . To see this, let  $\mathcal{B}_n$  be the set of all unordered pairs of nodes  $(\mathbf{u}, \mathbf{v})$  such that  $|\mathbf{u} - \mathbf{v}| > \ell(n)$ . Then the probability that none of the edges in the network is longer than  $\ell(n)$  is equal to the probability that none of these pairs is connected by an edge, which is

$$\Pr[\forall (\mathbf{u}, \mathbf{v}) \in \mathcal{E} : |\mathbf{u} - \mathbf{v}| \leq \ell(n)] = \left[ 1 - \sum_{(\mathbf{u}, \mathbf{v}) \in \mathcal{B}_n} p_n(\mathbf{u}, \mathbf{v}) \right]^{\gamma n}. \quad (23)$$

We now note the following points about the contact kernel:

- i) If  $\lim_{n \rightarrow \infty} \ell(n) = \infty$ , and recalling that the tail of  $\alpha(r)$  is nonincreasing, there is some  $n_1$  such that if  $n > n_1$  then for every  $(\mathbf{u}, \mathbf{v}) \in \mathcal{B}_n$  we have  $\alpha(|\mathbf{u} - \mathbf{v}|) \leq \alpha(\ell(n))$ .
- ii) If  $\lim_{n \rightarrow \infty} \ell(n) = \infty$  and given that  $\alpha(r) = O(e^{-cr})$ , there is some positive constant  $a$  and some  $n_2$  such that if  $n > n_2$  then  $\alpha(\ell(n)) \leq ae^{-c\ell(n)}$ .

So if we assume that  $\lim_{n \rightarrow \infty} \ell(n) = \infty$  and string together the inequalities in (i), (ii), and (19), we have, for sufficiently large  $n$ ,

$$p_n(\mathbf{u}, \mathbf{v}) \leq \frac{\kappa}{n} \alpha(|\mathbf{u} - \mathbf{v}|) \leq \frac{\kappa}{n} \alpha(\ell(n)) \leq \frac{\kappa a}{n} e^{-c\ell(n)}. \quad (24)$$

Combining this with Eq. (23) and noting that there are only  $n$  possible  $\mathbf{u}$  sites and  $n$  possible  $\mathbf{v}$  sites, so there are at most  $n^2$  terms in the sum in (23), we have

$$\Pr[\forall (\mathbf{u}, \mathbf{v}) \in \mathcal{E} : |\mathbf{u} - \mathbf{v}| \leq \ell(n)] \geq [1 - n\kappa a e^{-c\ell(n)}]^{\gamma n}. \quad (25)$$

Now let  $\ell(n) = (2/c) \log n$ , which satisfies our requirement that  $\lim_{n \rightarrow \infty} \ell(n) = \infty$ . Then the factor  $e^{-c\ell(n)}$  in (25) is just  $1/n^2$ . Combining this observation with (22), we arrive at

$$E[L_n] \geq \frac{1}{2} qc \left(1 - \frac{\kappa a}{n}\right)^{\gamma n} \frac{\sqrt{n}}{\log n}. \quad (26)$$

In the limit of large  $n$ , we have  $(1 - \kappa a/n)^{\gamma n} \rightarrow e^{-\gamma \kappa a}$  and hence  $E[L_n] = \Omega(\sqrt{n}/\log n)$  in this limit.  $\square$

Thus the network within our model, which consists of the network of physical disease transmission contacts plus the lattice of nearest-neighbor edges, does not display the small-world effect, and this immediately implies that the physical contact network alone also does not display the small-world effect. As described earlier, the final step in our argument is to point out, under the assumption that the edges in the network of social contacts are a subset of the edges in the network of physical contacts, that the social network will also not display the small-world effect, since removing edges from the network can only make paths longer, not shorter.

## V. DISCUSSION

Using a combination of empirical observation and mathematical reasoning, we have in this paper argued that the small-world effect—the occurrence of logarithmically short paths between most individuals in social networks—is a modern phenomenon, dating back no more than a few hundred years. In particular, the observation of slow, wave-like spread in historical disease

outbreaks such as the Black Death strongly suggests that the social world used to be large.

A number of further points seem worth noting. First, our calculations are all performed using an SI model in which infected individuals neither die nor recover from disease. However, with most human diseases, the Black Death included, individuals do recover or die, which could change the pattern of infection in various ways. In particular, when infected individuals remain infectious only for a limited time, the contact kernel for the disease is effectively truncated at a length-scale corresponding to the distance a person can travel in that time. Traveling on horseback, for example (the fastest form of land transportation in the 14th century), an individual carrying the Black Death could travel at most about 160 km in the four days for which victims of the disease remained infectious. In effect, therefore, the contact network would have no (or few) connections beyond this range. It seems unlikely, however, that this truncation affects our results. The Black Death advanced far slower than 40 km per day—its average speed of progress was perhaps about 2 km a day. Even on foot a human can travel an order of magnitude faster than this. This suggests that travel velocity was not the limiting factor in the spread of the disease. Another simplification in our calculation is the assumption of a uniform population. In reality, populations both then and now are highly nonuniform, being concentrated in metropolitan areas and sparse in rural areas. It would make an interesting topic for future study to incorporate realistically nonuniform distributions into the model, although it seems likely that one would then no longer be able to derive rigorous results.

We conclude with a question: if the global social network displays the small-world effect now but did not in the 14th century, when did things change? The occurrence of rapidly spreading pandemics in the 19th century suggests that the most substantial shift may have been the emergence around that time of relatively inexpensive means of long-range transportation, such as commercial railroads and passenger liners, but a full answer to the question will require detailed historical, geographical, and epidemiological studies before our understanding is complete.

## Acknowledgments

We thank Werner Horsthemke for helpful pointers to the literature on nonlocal reaction-diffusion equations. This work was supported by the US National Science Foundation under grants DMS-1107796 (TM and MEJN) and DMS-0927587 and PHY-1205219 (CRD), by the Marine Alliance for Science and Technology for Scotland under grant HR09011 (DL), and by the Michigan Society of Fellows (SAM).

- 
- [1] I. de Sola Pool and M. Kochen, Contacts and influence. *Social Networks* **1**, 1–48 (1978).
- [2] S. Milgram, The small world problem. *Psychology Today* **2**, 60–67 (1967).
- [3] J. Travers and S. Milgram, An experimental study of the small world problem. *Sociometry* **32**, 425–443 (1969).
- [4] D. J. Watts and S. H. Strogatz, Collective dynamics of ‘small-world’ networks. *Nature* **393**, 440–442 (1998).
- [5] R. Albert, H. Jeong, and A.-L. Barabási, Diameter of the world-wide web. *Nature* **401**, 130–131 (1999).
- [6] M. E. J. Newman, The structure of scientific collaboration networks. *Proc. Natl. Acad. Sci. USA* **98**, 404–409 (2001).
- [7] P. S. Dodds, R. Muhamad, and D. J. Watts, An experimental study of search in global social networks. *Science* **301**, 827–829 (2003).
- [8] J. Leskovec and E. Horvitz, Planetary-scale views on a large instant-messaging network. In *Proceedings of the 17th International Conference on the World Wide Web*, pp. 915–924, Association of Computing Machinery, New York (2008).
- [9] L. Backstrom, P. Boldi, M. Rosa, J. Ugander, and S. Vigna, Four degrees of separation. *Proceedings of the Third Annual ACM Web Science Conference (WebSci 2012)* pp. 33–42 (2012).
- [10] J. L. Moreno, *Who Shall Survive?* Beacon House, Beacon, NY (1934).
- [11] M. C. González, C. A. Hidalgo, and A.-L. Barabási, Understanding individual human mobility patterns. *Nature* **453**, 779–782 (2008).
- [12] A. Noulas, S. Scellato, R. Lambiotte, M. Pontil, and C. Mascolo, A tale of many cities: Universal patterns in human urban mobility. *PLoS ONE* **7**, 1–10 (2012).
- [13] J. M. Kleinberg, Navigation in a small world. *Nature* **406**, 845 (2000).
- [14] D. J. D. Earn, J. Dushoff, and S. A. Levin, Ecology and evolution of the flu. *TRENDS in Ecology & Evolution* **17**, 334–340 (2002).
- [15] C. W. J. Eliot, New evidence for the speed of the Roman Imperial Post. *Transactions of the American Philological Association* **82**, 136–148 (1951).
- [16] G. Chowell, H. Nishiura, and L. M. A. Bettencourt, Comparative estimation of the reproduction number of pandemic influenza from daily case notification data. *J. Roy. Soc. Interface* **4**, 155–166 (2007).
- [17] G. Christakos, R. Olea, and H.-L. Yu, Recent results on the spatiotemporal modelling and comparative analysis of Black Death and bubonic plague epidemics. *Public Health* **121**, 700–720 (2007).
- [18] D. Sherman and J. Salisbury, *The West in the World: Volume 1 to 1715*. McGraw-Hill, Boston, 3rd edition (2008).
- [19] S. Haensch, R. Bianucci, M. Signoli, M. Rajerison, M. Schultz, S. Kacki, M. Vermunt, D. A. Weston, D. Hurst, M. Achtman, E. Carniel, and B. Bramanti, Distinct clones of *Yersinia pestis* caused the Black Death. *PLoS Pathogens* **6**, e1001134 (2010).
- [20] D. Mollison, The rate of spatial propagation of simple epidemics. *Proceedings of the Sixth Berkeley Symposium on Mathematical Statistics and Probability* **3**, 579–614 (1972).
- [21] M. E. J. Newman, D. J. Watts, and S. H. Strogatz, Random graph models of social networks. *Proc. Natl. Acad. Sci. USA* **99**, 2566–2572 (2002).
- [22] F. Chung and L. Lu, The average distances in random graphs with given expected degrees. *Proc. Natl. Acad. Sci. USA* **99**, 15879–15882 (2002).
- [23] M. E. J. Newman and D. J. Watts, Scaling and percolation in the small-world network model. *Phys. Rev. E* **60**, 7332–7342 (1999).